forests

MDPI

Article

Assessing Rutting and Soil Compaction Caused by Wood Extraction Using Traditional and Remote Sensing Methods

Ikhyun Kim [1,†], Jaewon Seo [1,†], Heesung Woo [2,*] and Byoungkoo Choi [3,*]

[1] Department of Forestry and Environmental Systems, Kangwon National University, Chuncheon 24341, Republic of Korea; kih9281@kangwon.ac.kr (I.K.); tsl8760@kangwon.ac.kr (J.S.)
[2] Department of Forest Engineering, Resources & Management, Oregon State University, Corvallis, OR 97331, USA
[3] Division of Forest Science, Kangwon National University, Chuncheon 24341, Republic of Korea
* Correspondence: heesung.woo@oregonstate.edu (H.W.); bkchoi@kangwon.ac.kr (B.C.)
† These authors contributed equally to this work.

Abstract: Machine traffic during timber harvesting operations induces soil compaction, which is particularly evident in the formation of ruts. Visual inspection of rut formation is labor-intensive and limits the volume of data that can be collected. This study aims to contribute to the limited knowledge base regarding the extent of soil physical disturbance caused by machine traffic on steep slopes and to evaluate the utility of LiDAR and UAV photogrammetry techniques. The selected traffic trails included single-pass uphill, single-pass downhill, three-pass round trip, and five-pass round trip trails, with an average slope of 70.7%. Traditional methods were employed to measure rut depth using a pin board and to assess soil bulk density (BD) and soil porosity (SP) from soil samples. The results revealed that the average rut depth was 19.3 cm, while the deepest ruts were observed after a single pass (uphill: 20.0 cm; downhill: 22.7 cm), where BD and SP showed the most significant changes. This study provides a rare quantitative evaluation of the applicability of remote sensing methods in forestry by comparing surface height data collected via a pin board with that derived from a Mobile LiDAR System (MLS) and UAV photogrammetry using structure-from-motion (SfM). When compared to pin board measurements, the MLS data showed an R^2 value of 0.74 and an RMSE of 4.25 cm, whereas the SfM data had an R^2 value of 0.62 and an RMSE of 5.27 cm. For rut depth estimation, SfM (16.0 cm) significantly underestimated values compared to the pin board (19.3 cm) and MLS (19.9 cm). These findings not only highlight the potential and limitations of remote sensing methods for assessing soil disturbance in steep forest environments but also contribute to addressing the knowledge gaps surrounding the effects of soil compaction in steep terrain.

Keywords: mobile LiDAR system; UAV photogrammetry; digital elevation model; soil physical disturbance; timber harvesting

check for updates

Academic Editor: Nikolay S. Strigul

Received: 26 October 2024
Revised: 6 January 2025
Accepted: 6 January 2025
Published: 7 January 2025

Citation: Kim, I.; Seo, J.; Woo, H.; Choi, B. Assessing Rutting and Soil Compaction Caused by Wood Extraction Using Traditional and Remote Sensing Methods. *Forests* **2025**, *16*, 86. https://doi.org/10.3390/f16010086

Copyright: © 2025 by the authors. Licensee MDPI, Basel, Switzerland. This article is an open access article distributed under the terms and conditions of the Creative Commons Attribution (CC BY) license (https://creativecommons.org/licenses/by/4.0/).

1. Introduction

Mechanized timber production systems are a common and necessary practice to increase the efficiency of timber harvesting [1,2]. However, soil compaction and rutting, significant disturbances caused by the traffic of forestry machines, can have substantial impacts on forest ecosystems and sustainable forest management [3]. Understanding the extent and severity of these impacts is crucial for mitigating their negative consequences and implementing appropriate management practices.

In agriculture, technologies such as tire pressure adjustment and conservation tillage have been widely researched and implemented because soil compaction and crop loss

directly impact economic outcomes [4,5]. In contrast, forestry faces greater challenges in applying mitigation and prevention strategies due to the extensive and diverse terrain of work sites. Forest soils also present more complex issues because their natural recovery processes are slower, and forestry machinery is significantly heavier compared to agricultural machinery.

One of the most evident consequences of soil compaction is the formation of ruts, which are deep tracks created by the repeated passage of wheeled or tracked vehicles [6]. The formation of ruts increases soil density, resulting in soil hardening. Compacted soils exhibit increased penetration resistance, which can restrict root growth [7,8]. When soil penetration resistance exceeds 2.5 MPa, the root growth of many tree species is significantly impeded, as reported by Greacen and Sands [9] and Whalley et al. [10]. This level of soil penetration resistance is frequently reached during forest harvesting operations [6].

Soil compaction transforms macropores into micropores [11,12], reduces pore continuity, and decreases soil porosity (SP) [6]. As SP decreases, spaces previously open fill with soil solids. Roots rely on soil pore space to penetrate deeper into the soil, but in compacted soil, the limited pore space restricts root growth and development [13–15]. Restricted root growth prevents plants from obtaining nutrients and water from the soil, leading to stunted growth and potential seedling death [2,16]. In addition, changes in soil pore structure leads to a significant decline in soil aeration. Frey et al. [17] reported that soil air permeability in the 5–10 cm depth layer decreased by 96% when deep ruts formed after logging. Forest soils typically exhibit increasing CO_2 concentrations with depth due to reduced gas diffusion rates [18]. Magagnotti et al. [19] reported that in loamy sand soils, machine traffic during logging doubled CO_2 concentrations. Kim et al. [20] confirmed a substantial reduction in soil CO_2 diffusion and emissions following machine traffic. Gaertig et al. [21] also observed that CO_2 concentrations in compacted soils increased up to threefold, with root density significantly decreasing due to reduced soil gas permeability.

These problems vary depending on soil characteristics and operating conditions. Soil compaction tends to intensify with increasing slope because machine loads are more narrowly distributed on the ground. Agherkakli et al. [22] demonstrated that the increase in soil bulk density (BD) after logging was significantly greater on slopes steeper than 20% compared to slopes of less than 20%. Jourgholami et al. [23] reported that changes in BD, penetration resistance, and SP were highest on 0%–10% uphill slopes, followed by 10%–20% downhill and 0%–10% downhill slopes.

Most soil compaction occurs during the initial passes of machinery, with little additional compaction resulting from subsequent passes [24–26]. Soil compaction increases BD and, consequently, the bearing capacity of soil [27], enabling the topsoil layer to resist further compaction after the initial passes of machinery. Williamson and Neilsen [28] found that, on average, 62% of soil compaction in the 0–10 cm layer occurred after a single pass of machinery in clay and gravelly sandy soils, with minimal increases from subsequent passes. However, the extent of initial compaction varies depending on soil properties and operational conditions. Some studies have reported that soil compaction increases substantially with 5–10 machine passes but does not increase as significantly with more than 10 passes [23–26,28–30]. Contrarily, a meta-analysis by Nazari et al. [31] found that soil disturbance can peak with more than 20 passes of machinery. The authors also emphasized the lack of localized information on forest soil compaction caused by machinery traffic.

Soil compaction due to machinery traffic is influenced by various environmental and operational factors, such as soil texture, soil structure, the type of machinery used, and the number of machinery passes [6,32,33]. However, BD generally decreases with increasing soil depth [34–37]. This suggests that investigating surface soil layers is an efficient way to intuitively assess the effects of soil compaction.

Globally, various mitigation and prevention strategies have been researched and implemented to minimize soil disturbance from machinery traffic during forest operations. Commonly suggested measures include leaving harvesting residues on the ground to reinforce the topsoil [24,38], reducing contact pressure between machinery and soil [39–41], and planning appropriate logging designs [12,42,43]. However, these strategies, while effective in specific conditions, are not universally applicable across all forest sites. For instance, general measures may be inadequate in areas with complex mountainous terrains, unique rainfall patterns, or varying soil compositions. Thus, despite efforts to address and mitigate soil disturbance, reliable quantitative approaches are required to estimate the scope and severity of the problem [44].

Previous studies have implemented systematic sampling to evaluate soil disturbance in the field [36,45–47]. However, field-based soil disturbance monitoring on a large scale remains labor-intensive and costly [46]. To overcome these limitations, technical approaches utilizing high-resolution three-dimensional data are increasingly gaining attention [6,11,48]. Talbot and Astrup [49] reported that most studies assessing forest site disturbance rely on UAV photogrammetry, a cost-effective alternative to methods such as LiDAR. However, Talbot et al. [50] highlighted the lack of automated detection methods accurate enough to identify all soil disturbances. Furthermore, existing studies using various LiDAR systems or UAV-based photogrammetry for soil disturbance rarely provide empirical validation of the morphological detection accuracy of their methods. In steep or topographically complex forest areas, achieving high accuracy with LiDAR or photogrammetry remains challenging, requiring cautious application in such environments.

Advanced techniques developed in agricultural soil compaction research have demonstrated effectiveness in detecting subsurface compaction layers. Ground penetrating radar (GPR) and electromagnetic induction (EMI) are proven geophysical methods for this purpose [51,52]. Remote sensing and UAV-based photogrammetry have also been used to map soil compaction patterns over large areas with high spatial resolution [53,54]. Additionally, three-dimensional simulation models, such as finite element analysis, provide valuable insights into the mechanical behavior of soil under machine loads [55,56]. While these technologies are applicable to forestry, the unique environmental and operational conditions in forests necessitate tailored approaches, such as integrating LiDAR and photogrammetry.

Artificially afforested timber harvesting sites often have relatively gentle slopes. Strategies to minimize machinery traffic on steep slopes have led to a limited understanding of soil disturbance impacts in these areas. Ground-based mechanized harvesting methods are widely used on flat or slightly sloping terrain due to their safety and high labor productivity [57]. However, the operational range is expanding to steeper terrains with the use of winch-assisted skidders [58,59]. Additionally, some countries continue to harvest timber in steep environments where such operations are unavoidable. Nevertheless, information on the potential soil impacts in these steep areas remains scarce.

This study aims to (1) contribute to the limited knowledge base on the extent of soil disturbance caused by forestry machinery in steep forest regions and (2) evaluate and propose the utility of LiDAR and UAV photogrammetry techniques. Field sampling-based soil disturbance monitoring was conducted to understand the effects of machine traffic on soil compaction in steep terrains. Additionally, the accuracy of rut detection using LiDAR and UAV photogrammetry, applicable to routine forest management, was assessed.

2. Materials and Methods

2.1. Site Description and Experimental Design

The research for this study was conducted from 16 June to 20 June 2023, in the experimental forest of the Kangwon National University (37°50′18.6″ N, 127°50′0.38″ E; 615 m

elevation) in Gangwon Province, Republic of Korea. The climate in the study site was classified as a hot summer climate (Köppen Classification) with a mean annual air temperature of 11.6 °C (monthly averages ranged from 29.4 °C) and mean annual precipitation of 113.4 mm. During the study period (from 16 June to 20 June 2023), the mean air temperature and total precipitation at the site were 24.6 °C (22.8–26.9 °C) and 0.5 mm, respectively. The soil texture was loamy and classified as the Mui series based on U.S. soil taxonomy (coarse loamy, mixed, Typic Humudepts). The composition of the soil was 52.4% sand, 12.5% clay, and 35.2% silt. The average slope of the timber harvesting site was **53.4%**, while the average slope of the machine traffic trails was **70.7%**. Specifically, the average slope was **73.4%** on the single **uphill trail, 70.3%** on the single **downhill trail, 69.8%** on the **three-pass round trip trail**, and **69.2%** on the **five-pass round trip trail**.

The harvesting area, including the research site, was more of a deciduous stand with approximately 21% conifers (Table 1). There were a total of 1041 trees with an average tree volume of 0.45 m^3. The *Pinus koraiensis* were not harvested to prevent the spread of pine wilt disease.

Table 1. Vegetation description.

Species	Count (Ratio)	DBH (cm)
Larix kaempferi (Lamb.) Carriere	193 (18.5)	33.1
Quercus mongolica Fisch. ex Ledeb.	66 (6.3)	29.8
Quercus variabilis Blume	14 (1.3)	43.1
Other deciduous trees	721 (69.3)	17.5
Pinus koraiensis Siebold & Zucc.	47 (4.5)	13.1
Total	1041 (100)	21.3

DBH means average of diameter at breast height by tree species. Count means the number of trees by species in the harvesting area.

The research site was located in the timber harvesting area, and wood felling using a chainsaw ended on 9 June 2023. An excavator (HX 65 AMT, Hyundai®, Seoul, Republic of Korea) was used in wood throwing, which is the operation of throwing wood for timber transportation and loading. The tire of the excavator was a crawler type, and the weight of the excavator without load was 6.39 tons. The area where a single tire of the excavator directly pressed on the soil surface was approximately 380 mm wide and 1990 mm long. While driving in the harvesting area, the excavator threw the wood in the direction of the forest road located below the slope and organized it on the slope to prevent residues from being swept down (Figure 1b). During wood throwing, the excavator trail is not pre-designed and fluidly depends on the operator's subjectivity, and it does not pass only once on each trail. In this study, four treatments were imposed on the machine trail, where the experimental variables were a traffic frequency of 1, 3, and 5 excavator passes in the harvesting area (Figure 2). In addition, treatments with one pass were classified according to the direction of driving (uphill or downhill) (Figure 2). Plots were replicated three times, so a total of 12 plots were selected (Figure 2). In a selected plot, three survey lines were divided to assess the impacts of excavator traffic on soil during wood drawing (Figure 2). However, we excluded two survey lines because they experienced rapid soil disturbance due to a change in excavator direction during a single downhill drive (Figure 2).

2.2. Soil Physical Parameters

The impacts of grapple excavator traffic on the surface soil layer (0–10 cm depth) compaction were determined using dry BD and soil porosity (SP) measurements in comparison to the undisturbed area (Control) at the different conditions of traffic (Figure 2). After machine traffic, three soil samples were collected from inside both the left (LT) and right

(RT) sides in the wheel tracks (InT), three samples were collected between the tracks (BtwT), and three samples were collected in Control, where the undisturbed area from machine traffic was within 4 m of the trails. This resulted in a total of 12 samples per plot, except for one plot with a single downhill driving condition where only 4 samples were collected (Figure 2). A total of 136 soil samples were collected using a metal cylinder (100 m^3). BD was calculated as the dry weight (after a dry at 105 °C for 48 h) of the soil sample divided by the volume of the sampler. In addition, the difference in the weight of the soil samples before and after was used to calculate the volumetric SP. After assessing the normality of the data, a one-way analysis of variance (ANOVA) was conducted to compare BD and SP among the different treatments. Post hoc comparisons were then performed using the Bonferroni test to account for multiple comparisons. Data analyses were performed using SPSS statistical software version 26.0 (SPSS Inc., Chicago, IL, USA).

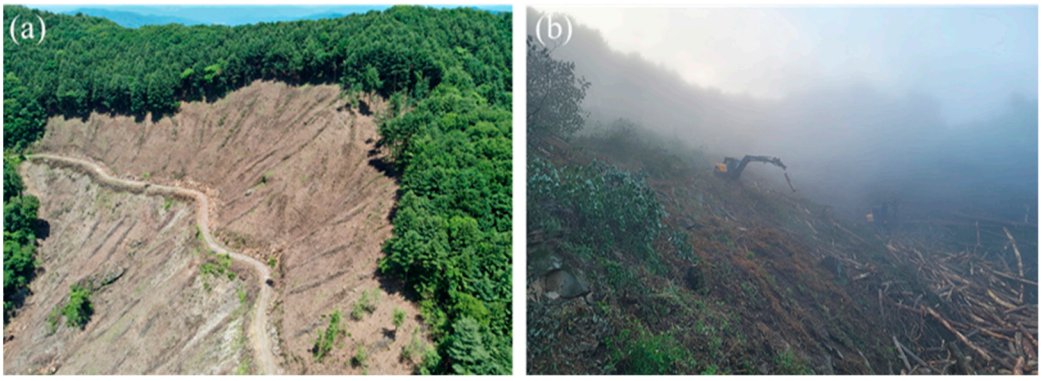


Figure 1. (**a**) Panorama view of study site in timber harvesting area and (**b**) wood-grab-equipped excavator during wood throwing.

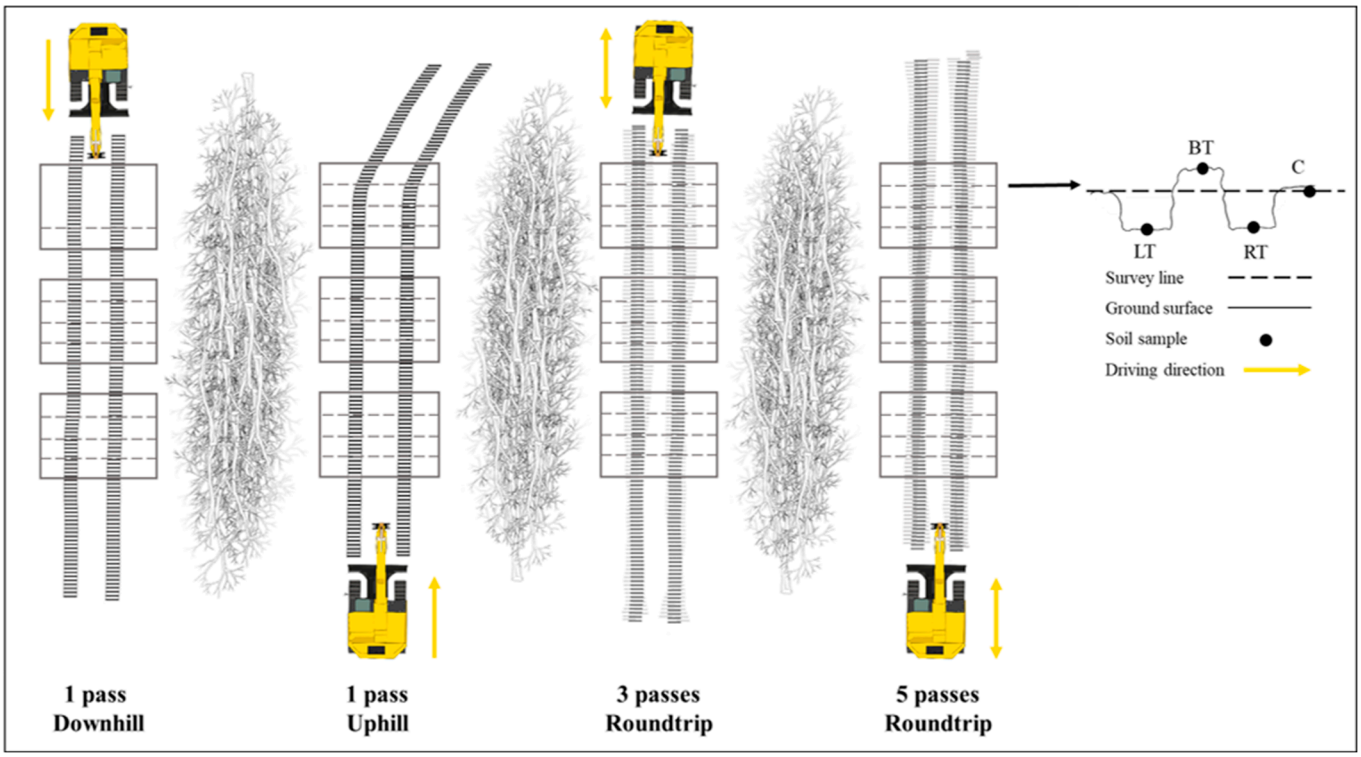


Figure 2. Schematic figure of the treatment in the research site. LT—left rack trail; RT—right rack trail; BT—between trail; C—control. Logging residues are piled up between the machine trail.

2.3. Rut Measurements

Two methods to perform a 3D soil reconstruction, derived by both mobile laser scanner (MLS) and UAV photogrammetry using structure-from-motion (SfM) algorithms, were applied to estimate rutting caused by machine traffic on forest soil. In addition, the ground profile was measured using a self-made pinboard to verify the soil rutting estimated by the two sensing technologies. Data collection and measurements were made in the same plots that were used to collect the other soil physical parameter data. In addition, following normality assessment, an ANOVA was used to analyze the differences in the measured and estimated soil rut depths across the various driving conditions and measurement methods. The Bonferroni correction test was used for post hoc comparisons. Data analyses were performed using SPSS statistical software version 26.0.

2.3.1. MLS Data Collection and Preprocess

A Hovermap (Emesent®, Queensland, Australia) simultaneous localization and mapping (SLAM)-based rotating LiDAR mapping device, was used as an MLS to collect the spatial data of plots within the research site (Figure 3b). The reported range of the sensor is 0.4 m to 100 m, with an accuracy of ±30 mm. The mapping accuracy in a general environment is ±20 mm and the LiDAR data acquisition speed is up to 300,000 points per sec. To collect data from the plots, the operator walked at a speed of approximately 40 cm/s, holding the instrument at a height of 1.3 m above the ground (Figure 3b). The operator trail was set to within 1.5 m of the boundary of the plot (Figure 3b). The operator started walking from the start point of the LiDAR run and ended the scanning by returning to the start point.



Figure 3. (**a**) Operator during capture of 2D images using UAV for performing SfM, (**b**) operator during laser scanning while walking, and (**c**) pinboard use for longitudinal profile acquisition for wheel track.

Collected LiDAR data were extracted and constructed to point cloud data (PCD) using Emesent software v1.6.2 (Emesent®). Extracted LiDAR data were processed using CloudCompare v2.11.1. (Retrieved from https://www.cloudcompare.org/). PCD was trimmed and cleaned of noise using the statistical outlier removal (SOR) tool based on 6 points and 1 standard deviation [60]. In addition, a filter noise tool was used to remove the noise of LiDAR data. In each plot, the ground surface profile was extracted using Agisoft Metashape Professional (Version 1.5.1 build 7618, Retrieved from http://www.agisoft.com/downloads/installer/) based on the cross section by delimiting a polyline identical to the survey line in the acquired LiDAR data.

2.3.2. SfM Data Collection and Preprocess

The 3D construction of the research site was based on 2D images applying SfM. In this study, these images were collected using a 2D camera (Zenmuse H20T, DJI Enterprise,

Shenzhen, China) with 4056 × 3040 pixels. The camera was mounted on a UAV (Matrice 300, DJI Enterprise). The designed flight path totaled 2255 m, and the mapping area was approximately 3 ha (30,282 m^2). Automated UAV flight was performed for image acquisition. The flight was performed at 3 m/s at an altitude of 70 m, with a front and side overlap of 90% and a margin of 20 m. A total of 297 images were acquired during the automated flight.

The SfM method was applied to obtain 3D point clouds of the research site. The 2D images were aligned using Agisoft Metashape Professional (Version 1.5.1 build 7618) and a dense point cloud was generated (Figure 4). We extracted a ground surface profile for the survey line, similar to the one applied to the LiDAR data.

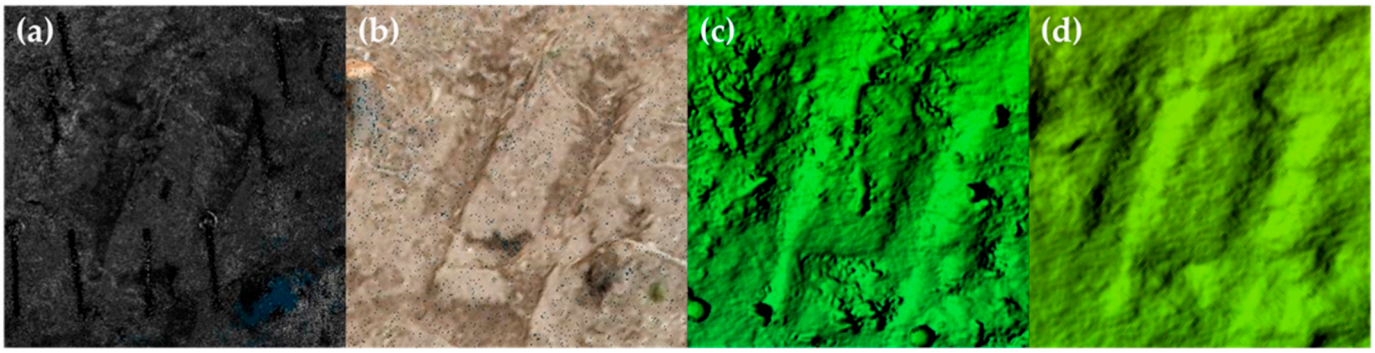


Figure 4. Acquisition data using MLS and data processing to apply the SfM algorithm. Examples of zoomed-in views of (**a**) point cloud data obtained from MLS and (**b**) point cloud data (PCD) generated using SfM on wheel tracks. The digital elevation model (DEM) generated using (**c**) PCD of MLS and (**d**) PCD of SfM for the same location of PCD.

2.3.3. Validation Data Collection Using Pinboard

The accuracy of the detection of morphological features of the ground surface using MLS and SfM was compared with the ground truth data (field-measured surface profile using pinboard) at the survey lines (Figure S1). Measurements with the pinboard were only performed on survey lines delineated within the plot (Figure 3c). Steel poles were installed at each end of the survey line, and the poles were connected by nylon ropes to identify the survey line (Figure 3b). The pinboard is made of 1 mm diameter steel pins spaced 1 cm apart, so that when the bottom of the pins touches the ground, they can move fluidly with the shape of the ground (Figure 3c). A spirit level was placed on the back of the pinboard to ensure that the image was acquired while the pinboard was level when viewed from the front (Figure 3c). Yellow masking tape was wrapped around the top of the steel pins so that the profile data could be obtained by reading the scale attached to the pinboard (Figure 3c). Linear regression and root mean square error (RMSE) analyses were performed to verify the accuracy of the soil profiles obtained using MLS and SfM.

3. Results and Discussion

3.1. Rut Formation After Forestry Machine Traffic

Following the passage of forestry machinery, each wheel track had an average rut of 19.3 cm depth, as measured with a pinboard (Figure 5). The deepest rut measured 22.7 cm after a single downhill pass of the machinery, and the second deepest was 20.0 cm after an uphill pass (Figure 5). The direction of forestry machine seemed not to significantly affect rut formation ($p > 0.05$, Figure 5). These results are consistent with the findings of Marra et al. [61], who reported that extraction direction did not affect the severity of soil damage. However, they recommended that a downhill pass should preferably be used to reduce soil compaction. Due to driving stability issues on extreme slopes, the machinery moved

slower downhill than uphill in the study area. Reducing speed on steep slopes can increase soil vibration and cause severe soil compaction compared to flat terrains [62,63].

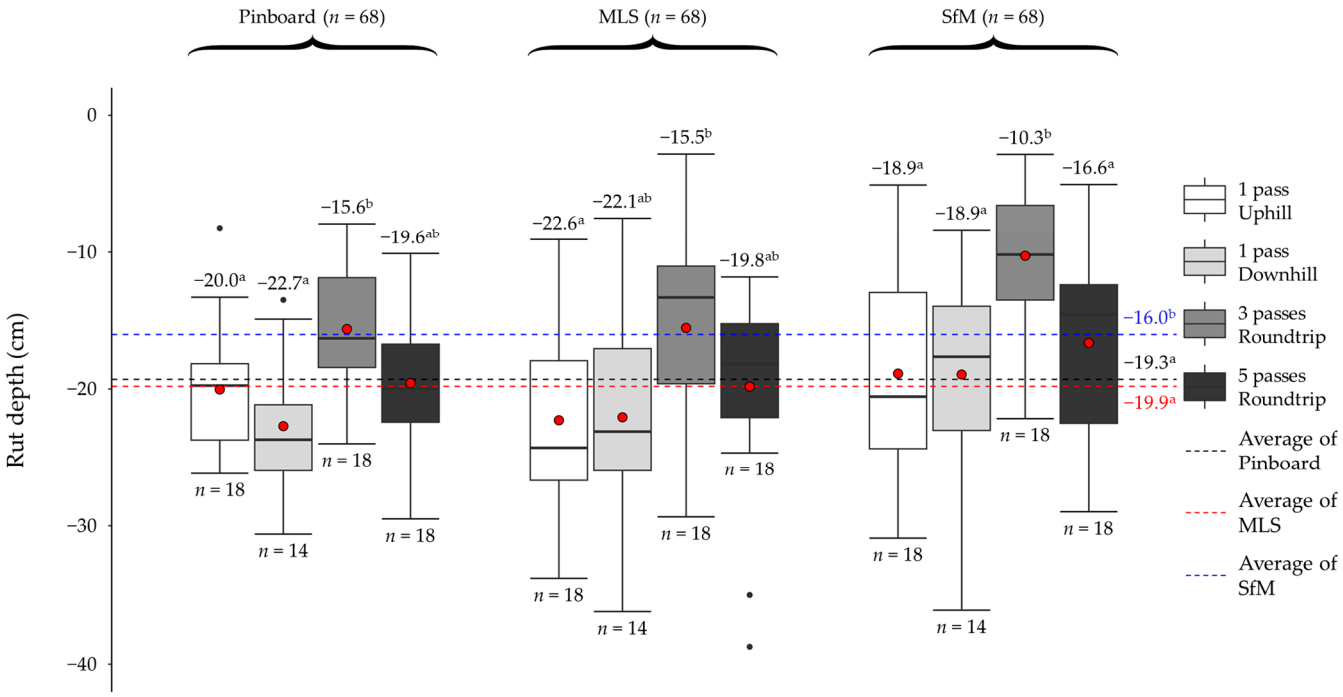


Figure 5. Rut formation by forestry machine driving conditions (intensity and direction of driving) for each measurement method (MLS and SfM). Red points indicate average values and bold black horizontal lines within each boxplot indicate median values. Different letters represent significant differences in soil rut depth among machine driving conditions and measurement methods, respectively, at $p < 0.05$.

The shallowest rut, measuring 15.6 cm deep, was formed after three passes of the machinery, significantly shallower than after a single pass ($p = 0.00$, Figure 5). Moreover, the depth of the rut after the machinery passed five times was 19.6 cm, and this is shallower than the depth of the rut after a single pass, but is not significant ($p > 0.05$, Figure 5). Rut formations were observed to be deeper where the forestry machine was driven once than where it had round trips. These results may be attributed to the displacement and mixing of the topsoil layer caused by operations on steep slopes [64,65]. In addition to the slope gradient and intensity and direction of the forestry machine traffic, the severity of rut formation depends on other factors such as soil texture, moisture, and organic matter [6]. The factors influencing soil disturbance after forestry machine traffic may vary even within the same site due to soil variability [66,67]. Therefore, additional variables need to be investigated to accurately determine the impact of forestry machine traffic on soil disturbance.

To visually assess rut formation after forestry machine traffic, a soil disturbance classification by McMahon [45] was applied. According to the classification, all forestry machine driving condition treatments were classified as Code 10, except for the three passes round trip, which was classified as Code 9 (Table S1). This indicates that the visual soil disturbance observed under all driving conditions corresponded to 'Deep disturbance'.

These results indicate that initial machinery traffic significantly impacts the soil sufficiently to be visually identified. However, additional passes do not necessarily deepen the wheel tracks as the surface soil is displaced or compacted [1]. Morphological changes like rut formation due to forestry machinery traffic suggest soil disturbance and can alter the physical properties of the soil.

3.2. Changes in Soil Physical Properties After Forestry Machine Traffic

It was observed that the BD increased in all forestry machinery traffic lanes at both BtwT and InT compared to the Control (Figure 6). In the four traffic lanes at InT, there was a statistically significant increase in average BD by 19.1% compared to the Control (p = 0.00), and BtwT also increased by 5.4% compared to the Control, although it was not significant (p > 0.05, Figure 6). Similarly to our findings, Ampoorter et al. [3] reported that BD at BtwT and InT increased after forestry machine traffic at soil depths of 0–50 cm compared to the Control. These results suggest that the soil disturbance caused by forestry machine traffic was not limited to machine tracks [68].

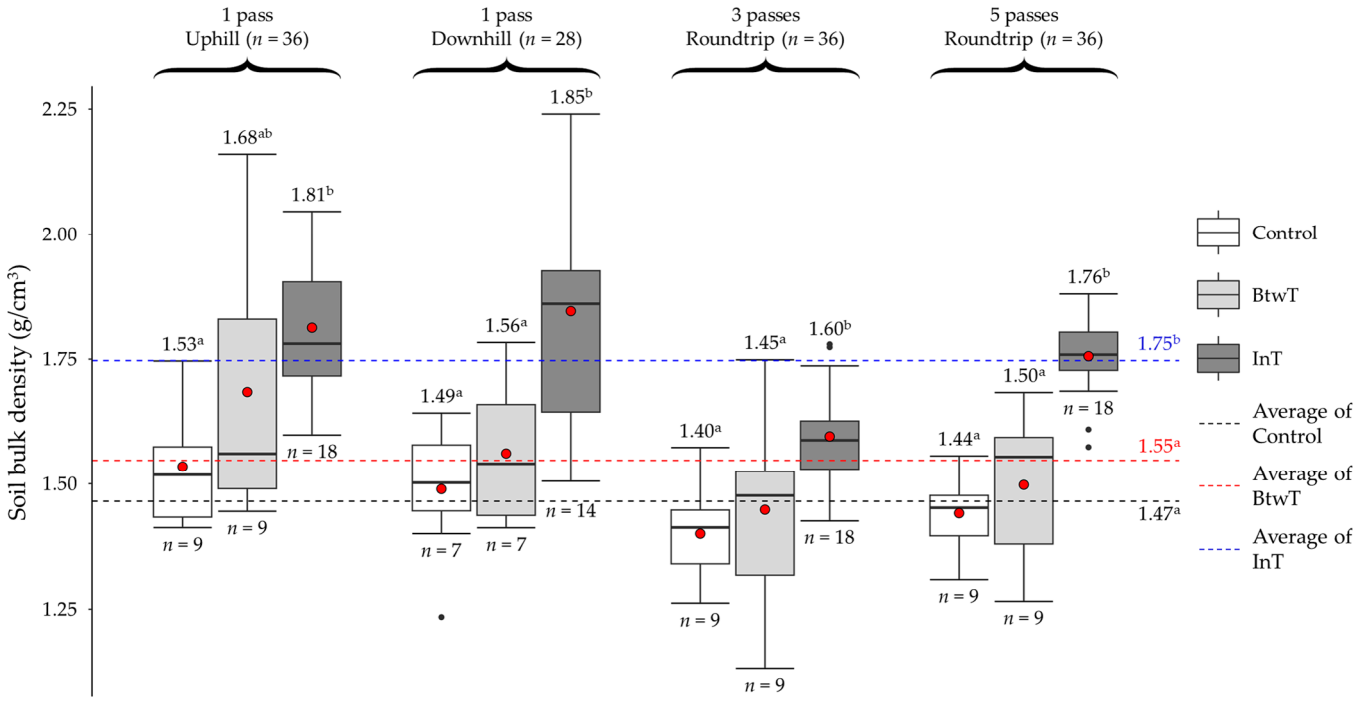


Figure 6. Soil bulk density (BD) by forestry machine driving conditions and positions. Red points indicate average values, and bold black horizontal lines within each boxplot indicate median values. Different letters with top of each box represent significant difference in BD among position in each machine track at p < 0.05.

When the forestry machinery passed once, there was an increase of 24.2% in BD at InT during downhill travel, and an increase of 18.3% during uphill travel (Figure 6). After five passes of the machinery, there was an increase of 22.2% in BD at InT, and the smallest increase of 14.3% occurred at InT after three passes of the machinery (Figure 6). The changing trend in BD after the machinery passage closely corresponded with the depth of the formed ruts and, similar to rut formation, a single pass was sufficient to cause an increase in BD [3]. Although the degree of soil compaction depends on BD prior to forestry machine traffic [16], BD increased rapidly on steep slopes even after a single pass of the forestry machine [69]. An increase in BD has a significant impact on the quality of seedlings [70]. For fine-textured soils, BD in the range of approximately 1.4 to 1.6 g/cm^3 is considered the critical level for root penetration, whereas for coarse-textured soils, the critical level of BD is 1.75 g/cm^3 [14].

As bulk density increases, SP decreases [6]. Forest soils, due to their fragile structure and high porosity, are particularly susceptible to compaction [48]. After mechanical traffic, soil compaction can reduce SP by up to 60% [3,6,71]. The limited pore space in compacted soil can inhibit the growth and development of plant roots [72] and affect the availability of

water, minerals, and soil air [20,73]. While not all soil compaction is detrimental to plant growth [74], soil disturbance is a crucial consideration in long-term forest management.

SP was significantly reduced by 23.7% in all InT compared to the Control (p = 0.00), and although not significant, SP was also reduced by 6.9% in BtwT compared to the Control (p > 0.05, Figure 7). Furthermore, while other driving conditions reduced SP in BtwT by up to 6.2% compared to Control, a one-time upward drive reduced SP in BtwT by 13.5%. These trends were also found in BD (Figure 6). Solgi et al. [75] evaluated the effects of skidder traffic on BD and SP in WT and BtwT under mountainous forest conditions and, similar to our results for one-pass uphill travel, the results showed that after a single pass of the skidder, BD increased and SP decreased in WT and BtwT compared to areas 4 m away from WT.

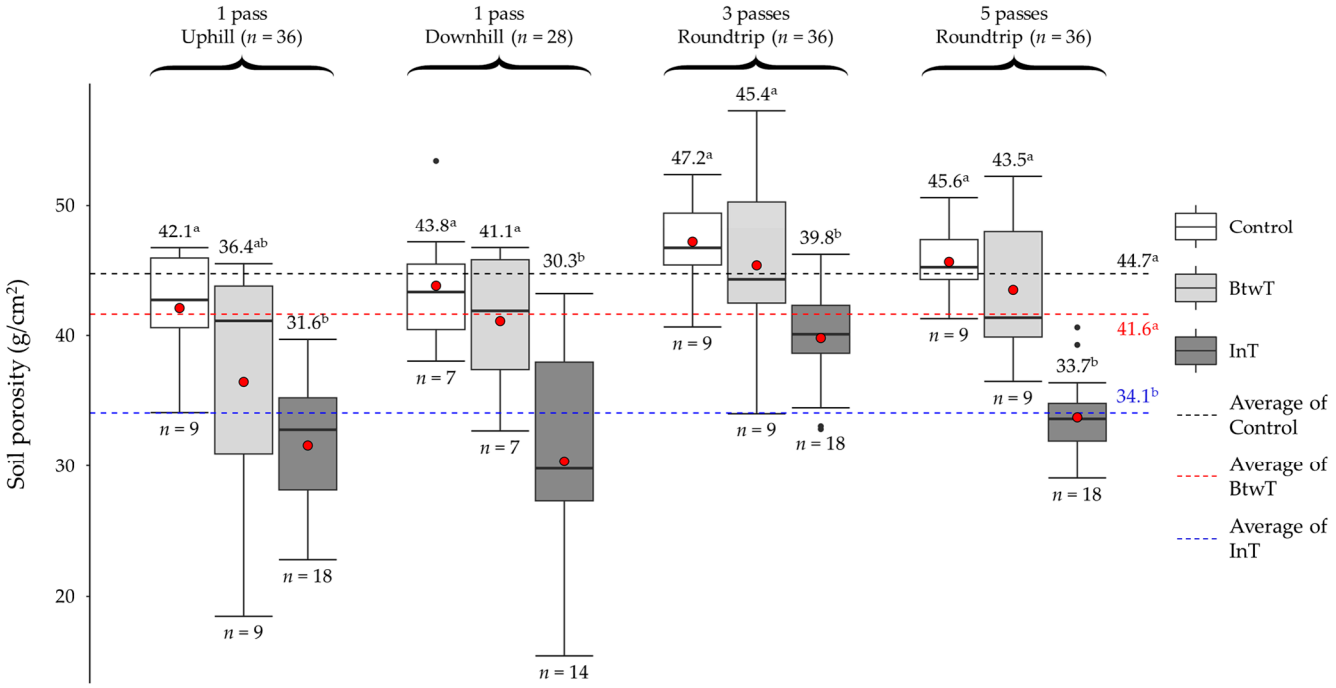


Figure 7. Soil porosity (SP) by forestry machine driving conditions and positions. Red points indicate average values, and bold black horizontal lines within each boxplot indicate median values. Different letters indicate significant differences in SP among position in each machine track at p < 0.05.

The greatest reduction in SP, 30.8%, occurred in InT after a single downhill pass of the machinery, which seems to be associated with deep rut formation and a significant increase in BD (Figure 7). However, after five passes of the machinery, SP in InT decreased by 26.1%, the second greatest reduction, showing a trend slightly different from that of rut depth and BD increase (Figure 7). The impact of soil compaction due to machinery traffic can be influenced by soil characteristics such as soil moisture content, but SP may continuously decrease as traffic frequency increases [71,76].

However, according to the parameters investigated in this study to assess the impact of soil compaction, it appears that the greatest impact on the soil occurred after a single pass of the machinery. Previous studies have also reported that initial machinery traffic significantly affects the soil [1,77]. Regardless of machinery type, BD can increase by up to 50% within the first three passes [3,63]. Particularly in steep terrains, soil compaction is more likely to occur, hence ground-based logging operations are best suited to slopes of less than 30% [78].

3.3. Soil Disturbances Assessment with Remote Sensing

Many previous studies agree on the necessity of designing forest roads and machine traffic trails rationally. However, some authors propose reducing the number of traffic trails to concentrate the impacts of machine traffic on a limited surface [62]. In contrast, others recommend designing more traffic trails to distribute soil compaction more evenly by limiting the number of passes on a single trail [79]. Nevertheless, it is critical to prevent machines from deviating from the designated trails in either case. Building three-dimensional data on the target area can be highly useful for assessing the successful implementation of planned operations and understanding the spatial extent of soil disturbance.

The accuracy of soil surface estimation was higher for the MLS-based data than for the SfM-based data, with an average of 7.75 mm pixel^{-1} for MLS and 2.33 cm pixel^{-1} for SfM. Using MLS, SfM, and a pinboard, a total of 68 profile lines were generated, from which 4494 soil surface height data points were acquired for each method. To validate the MLS- and SfM-based data, linear models were fitted to the soil surface height data, which were obtained using the pinboard. When comparing the surface estimates made using MLS with the pinboard data, the R^2 value was 0.74 and the slope of the linear model was 0.98 (p = 0.00, Figure 8). It was difficult to hold and move the MLS on steep slopes when detecting the soil surface with the MLS. This may have affected the R^2 value of the MLS. The R^2 value between the SfM-based data and the pinboard data were 0.65 and the slope of the linear model was 0.82 (p = 0.00, Figure 8). However, the SfM-based data appeared to be at a disadvantage due to blurring and distortions in detecting complex and irregular terrains [80–82].

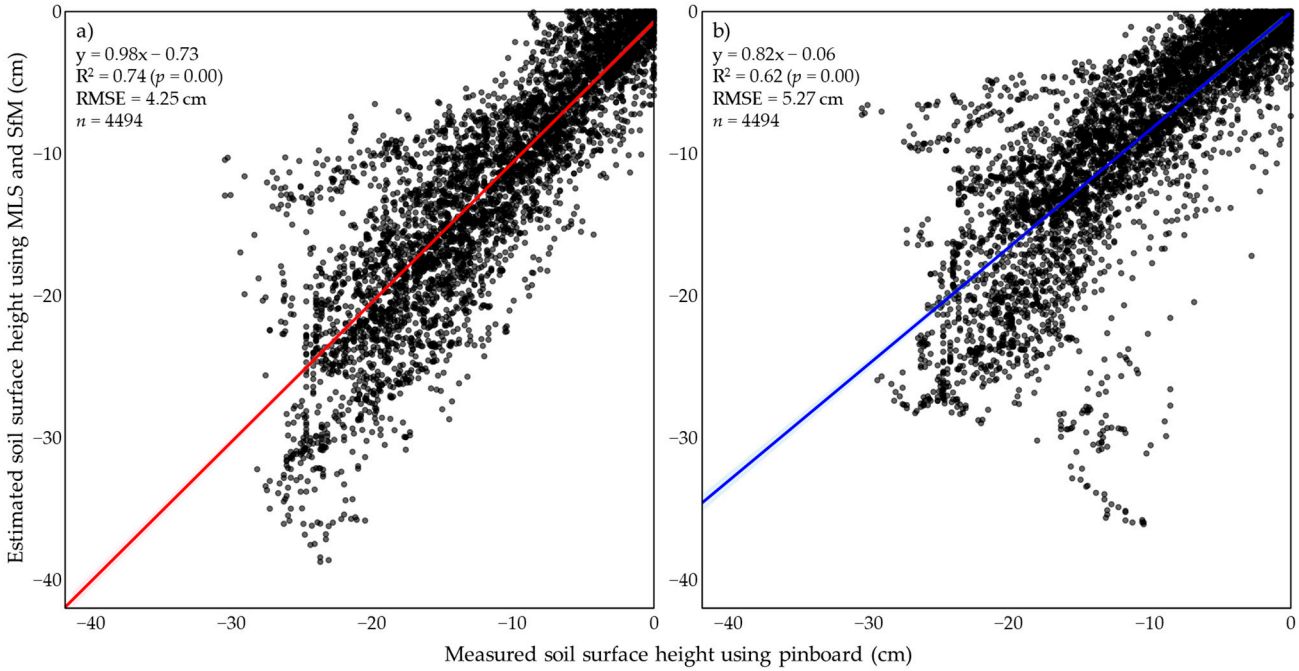


Figure 8. Linear models comparing soil surface height measured with the pinboard to soil surface height estimated with MLS (**a**) and SfM (**b**) at sites where soil disturbance was caused by machine traffic.

The RMSE for the soil surface height estimated by MLS was 4.25 cm, whereas the RMSE for SfM was 5.27 cm (Figure 8). The tendency to over- or underestimate may be due to collection and processing errors in remote sensing data [83,84]. Overall, it was confirmed that morphological distortions or blurring were more frequently occurring in complex forest terrains when using SfM compared to LiDAR.

Foldager et al. [85] conducted experiments on a flat testbed where they created artificial furrows and scanned the ground surface using terrestrial LiDAR. The results showed up to a 41% difference in the cross-sectional area measurements between the pinboard and the LiDAR. Additionally, various studies have utilized LiDAR and SfM for scanning surface data in diverse landscapes. Moreover, there have been reports of studies aiming to assess the impact of forestry machinery using LiDAR and SfM [61,86–88]. However, cases of verifying scanned surface data with field measurements are extremely rare. This is particularly true in steep or complex terrains, where accuracy verification of surface disturbance data scanned using LiDAR and SfM is almost non-existent.

4. Conclusions

This study aimed to enhance the understanding of soil physical disturbance and rut formation caused by machine traffic on steep slopes during timber harvesting operations, while evaluating the applicability of LiDAR and UAV photogrammetry for assessing such impacts. The results showed that a single machine pass led to a more significant increase in bulk density and a sharper reduction in porosity compared to multiple passes, such as three or five. These findings highlight that minimizing the number of machine trails is a more effective strategy to mitigate soil compaction impacts in steep terrains.

Regarding the accuracy of remote sensing techniques, mobile LiDAR demonstrated a high level of reliability in estimating rut depth, with an average value of 19.9 cm that was statistically comparable to field-measured depths of 19.3 cm. In contrast, UAV photogrammetry significantly underestimated rut depth at 16.0 cm compared to both field measurements and LiDAR data. While UAV photogrammetry exhibited limitations in accurately estimating rut depth, it showed potential for identifying the spatial extent of disturbed areas, suggesting its applicability with further technical refinement.

Despite these advancements, challenges remain. Both mobile LiDAR and UAV photogrammetry exhibited notable data dispersion, with RMSE values of 4.25 cm and 5.27 cm, respectively. These errors, partially stemming from verification processes, emphasize the need for improving measurement precision. Furthermore, this study was limited to the topsoil layer (0–10 cm), leaving subsoil effects unexamined, which could provide a more comprehensive perspective on soil disturbance dynamics in future research.

In conclusion, this study supports the strategy of reducing the number of machine trails to effectively minimize soil compaction on steep slopes. Moreover, it underscores the potential of mobile LiDAR for accurately detecting rut formation and highlights the promise of UAV photogrammetry for identifying disturbed areas. With further technological advancements, these tools could significantly enhance soil disturbance assessments in steep forest environments.

Supplementary Materials: The following supporting information can be downloaded at: https://www.mdpi.com/article/10.3390/f16010086/s1, Table S1. Visual soil disturbance classification by McMahon [45], Figure S1. Optimal soil surface profile by machine driving conditions and positions for each measurement methods.

Author Contributions: Conceptualization, B.C., H.W., and I.K.; methodology, I.K. and H.W.; software, I.K., J.S., and H.W.; validation, B.C., I.K., H.W., and J.S.; formal analysis, I.K. and J.S.; investigation, I.K. and J.S.; resources, B.C. and H.W.; data curation, I.K. and J.S.; writing—original draft preparation, I.K. and J.S.; writing—review and editing, B.C. and H.W.; visualization, I.K. and J.S.; supervision, B.C. and H.W.; project administration, B.C.; funding acquisition, B.C. All authors have read and agreed to the published version of the manuscript.

Funding: This research was supported by the National Research Foundation of Korea (NRF), funded by the Korean government (No. NRF-2021R1A2C2008002).

Data Availability Statement: The data presented in this study are available on reasonable request from the corresponding authors. Data related to the study have been presented within the article.

Conflicts of Interest: The authors declare that they have no competing financial interest related to personal relationships that could have influenced the work reported in this study.

References

1. Allman, M.; Dudáková, Z.; Jankovský, M.; Vlčková, M.; Juško, V.; Tomčík, D. Soil compaction after increasing the number of wheeled tractors passes on forest soils in west Carpathians. *Forests* **2022**, *13*, 109. [CrossRef]
2. Ampoorter, E.; De Schrijver, A.; Van Nevel, L.; Hermy, M.; Verheyen, K. Impact of mechanized harvesting on compaction of sandy and clayey forest soils: Results of a meta-analysis. *Ann. For. Sci.* **2012**, *69*, 533–542. [CrossRef]
3. Ampoorter, E.; Goris, R.; Cornelis, W.; Verheyen, K. Impact of mechanized logging on compaction status of sandy forest soils. *For. Ecol. Manag.* **2007**, *241*, 162–174. [CrossRef]
4. Bailey, A.; Raper, R.; Way, T.; Burt, E.; Johnson, C. Soil stresses under a tractor tire at various loads and inflation pressures. *J. Terramechanics* **1996**, *33*, 1–11. [CrossRef]
5. Afzalinia, S.; Zabihi, J. Soil compaction variation during corn growing season under conservation tillage. *Soil Tillage Res.* **2014**, *137*, 1–6. [CrossRef]
6. Cambi, M.; Certini, G.; Neri, F.; Marchi, E. The impact of heavy traffic on forest soils: A review. *For. Ecol. Manag.* **2015**, *338*, 124–138. [CrossRef]
7. Taylor, H.; Brar, G. Effect of soil compaction on root development. *Soil Tillage Res.* **1991**, *19*, 111–119. [CrossRef]
8. Wästerlund, I. Compaction of till soils and growth tests with Norway spruce and Scots pine. *For. Ecol. Manag.* **1985**, *11*, 171–189. [CrossRef]
9. Greacen, E.L.; Sands, R. Compaction of forest soils. A review. *Soil Res.* **1980**, *18*, 163–189. [CrossRef]
10. Whalley, W.R.; Dumitru, E.; Dexter, A. Biological effects of soil compaction. *Soil Tillage Res.* **1995**, *35*, 53–68. [CrossRef]
11. Berli, M.; Kirby, J.; Springman, S.; Schulin, R. Modelling compaction of agricultural subsoils by tracked heavy construction machinery under various moisture conditions in Switzerland. *Soil Tillage Res.* **2003**, *73*, 57–66. [CrossRef]
12. Horn, R.; Vossbrink, J.; Peth, S.; Becker, S. Impact of modern forest vehicles on soil physical properties. *For. Ecol. Manag.* **2007**, *248*, 56–63. [CrossRef]
13. Tracy, S.R.; Black, C.R.; Roberts, J.A.; Mooney, S.J. Soil compaction: A review of past and present techniques for investigating effects on root growth. *J. Sci. Food Agric.* **2011**, *91*, 1528–1537. [CrossRef]
14. Kozlowski, T. Soil compaction and growth of woody plants. *Scand. J. For. Res.* **1999**, *14*, 596–619. [CrossRef]
15. Hansson, L.; Šimůnek, J.; Ring, E.; Bishop, K.; Gärdenäs, A.I. Soil compaction effects on root-zone hydrology and vegetation in boreal forest clearcuts. *Soil Sci. Soc. Am. J.* **2019**, *83*, S105–S115. [CrossRef]
16. Powers, R.F.; Scott, D.A.; Sanchez, F.G.; Voldseth, R.A.; Page-Dumroese, D.; Elioff, J.D.; Stone, D.M. The North American long-term soil productivity experiment: Findings from the first decade of research. *For. Ecol. Manag.* **2005**, *220*, 31–50. [CrossRef]
17. Frey, B.; Kremer, J.; Rüdt, A.; Sciacca, S.; Matthies, D.; Lüscher, P. Compaction of forest soils with heavy logging machinery affects soil bacterial community structure. *Eur. J. Soil Biol.* **2009**, *45*, 312–320. [CrossRef]
18. Certini, G.; Corti, G.; Agnelli, A.; Sanesi, G. Carbon dioxide efflux and concentrations in two soils under temperate forests. *Biol. Fertil. Soils* **2003**, *37*, 39–46. [CrossRef]
19. Magagnotti, N.; Spinelli, R.; Güldner, O.; Erler, J. Site impact after motor-manual and mechanised thinning in Mediterranean pine plantations. *Biosyst. Eng.* **2012**, *113*, 140–147. [CrossRef]
20. Kim, I.; Han, S.-K.; Acuna, M.; Woo, H.; Oh, J.-H.; Choi, B. Effect of heavy machine traffic on soil CO2 concentration and efflux in a Pinus Koraiensis thinning stand. *Forests* **2021**, *12*, 1497. [CrossRef]
21. Gaertig, T.; Schack-Kirchner, H.; Hildebrand, E.E.; v Wilpert, K. The impact of soil aeration on oak decline in southwestern Germany. *For. Ecol. Manag.* **2002**, *159*, 15–25. [CrossRef]
22. Agherkakli, B.; Najafi, A.; Sadeghi, S. Ground based operation effects on soil disturbance by steel tracked skidder in a steep slope of forest. *J. For. Sci.* **2010**, *56*, 278–284. [CrossRef]
23. Jourgholami, M.; Soltanpour, S.; Etehadi Abari, M.; Zenner, E.K. Influence of slope on physical soil disturbance due to farm tractor forwarding in a Hyrcanian forest of northern Iran. *iforest-Biogeosciences For.* **2014**, *7*, 342. [CrossRef]
24. Han, H.-S.; Page-Dumroese, D.; Han, S.-K.; Tirocke, J. Effects of slash, machine passes, and soil moisture on penetration resistance in a cut-to-length harvesting. *Int. J. For. Eng.* **2006**, *17*, 11–24. [CrossRef]
25. Wang, L. Assessment of animal skidding and ground machine skidding under mountain conditions. *J. For. Eng.* **1997**, *8*, 57–64.
26. Wallbrink, P.; Roddy, B.; Olley, J. A tracer budget quantifying soil redistribution on hillslopes after forest harvesting. *Catena* **2002**, *47*, 179–201. [CrossRef]
27. Hillel, D. *Environmental Soil Physics*; Academic Press: San Diego, CA, USA, 1998.

28. Williamson, J.; Neilsen, W. The influence of forest site on rate and extent of soil compaction and profile disturbance of skid trails during ground-based harvesting. *Can. J. For. Res.* **2000**, *30*, 1196–1205. [CrossRef]
29. Gent, J., Jr.; Ballard, R.; Hassan, A.; Cassel, D. Impact of harvesting and site preparation on physical properties of Piedmont forest soils. *Soil Sci. Soc. Am. J.* **1984**, *48*, 173–177. [CrossRef]
30. Brais, S.; Camire, C. Soil compaction induced by careful logging in the claybelt region of northwestern Quebec (Canada). *Can. J. Soil Sci.* **1998**, *78*, 197–206. [CrossRef]
31. Nazari, M.; Arthur, E.; Lamandé, M.; Keller, T.; Bilyera, N.; Bickel, S. A meta-analysis of soil susceptibility to machinery-induced compaction in Forest ecosystems across global climatic zones. *Curr. For. Rep.* **2023**, *9*, 370–381. [CrossRef]
32. Laffan, M.; Jordan, G.; Duhig, N. Impacts on soils from cable-logging steep slopes in northeastern Tasmania, Australia. *For. Ecol. Manag.* **2001**, *144*, 91–99. [CrossRef]
33. Naghdi, R.; Solgi, A.; Labelle, E.R.; Zenner, E.K. Influence of ground-based skidding on physical and chemical properties of forest soils and their effects on maple seedling growth. *Eur. J. For. Res.* **2016**, *135*, 949–962. [CrossRef]
34. Koolen, A.; Lerink, P.; Kurstjens, D.; Van den Akker, J.; Arts, W. Prediction of aspects of soil-wheel systems. *Soil Tillage Res.* **1992**, *24*, 381–396. [CrossRef]
35. McNabb, D.; Startsev, A.; Nguyen, H. Soil wetness and traffic level effects on bulk density and air-filled porosity of compacted boreal forest soils. *Soil Sci. Soc. Am. J.* **2001**, *65*, 1238–1247. [CrossRef]
36. Han, S.-K.; Han, H.-S.; Page-Dumroese, D.S.; Johnson, L.R. Soil compaction associated with cut-to-length and whole-tree harvesting of a coniferous forest. *Can. J. For. Res.* **2009**, *39*, 976–989. [CrossRef]
37. Jansson, K.; Johansson, J. Soil changes after traffic with a tracked and a wheeled forest machine: A case study on a silt loam in Sweden. *For. Int. J. For. Res.* **1998**, *71*, 57–66. [CrossRef]
38. McDonald, T.P.; Seixas, F. Effect of slash on forwarder soil compaction. *J. For. Eng.* **1997**, *8*, 15–26.
39. Alakukku, L.; Weisskopf, P.; Chamen, W.; Tijink, F.; Van Der Linden, J.; Pires, S.; Sommer, C.; Spoor, G. Prevention strategies for field traffic-induced subsoil compaction: A review: Part 1. Machine/soil interactions. *Soil Tillage Res.* **2003**, *73*, 145–160. [CrossRef]
40. Sakai, H.; Nordfjell, T.; Suadicani, K.; Talbot, B.; Bøllehuus, E. Soil compaction on forest soils from different kinds of tires and tracks and possibility of accurate estimate. *Croat. J. For. Eng. J. Theory Appl. For. Eng.* **2008**, *29*, 15–27.
41. Myhrman, D. Factors influencing rut formation from forestry machines. In Proceedings of the 10th International conference of the ISTVS, Kobe, Japan, 20–24 August 1990.
42. Chamen, T.; Alakukku, L.; Pires, S.; Sommer, C.; Spoor, G.; Tijink, F.; Weisskopf, P. Prevention strategies for field traffic-induced subsoil compaction: A review: Part 2. Equipment and field practices. *Soil Tillage Res.* **2003**, *73*, 161–174. [CrossRef]
43. Schäffer, J.; Buberl, H.; von Wilpert, K. Deformation damages in forest topsoils—An assessment based on Level-I soil monitoring data from Baden-Württemberg (SW Germany). *J. Plant Nutr. Soil Sci.* **2012**, *175*, 24–33. [CrossRef]
44. McDonald, T.; Carter, E.; Taylor, S. Using the global positioning system to map disturbance patterns of forest harvesting machinery. *Can. J. For. Res.* **2002**, *32*, 310–319. [CrossRef]
45. McMahon, S. Accuracy of two ground survey methods for assessing site disturbance. *J. For. Eng.* **1995**, *6*, 27–33. [CrossRef]
46. Reeves, D.A.; Reeves, M.C.; Abbott, A.M.; Page-Dumroese, D.S.; Coleman, M.D. A detrimental soil disturbance prediction model for ground-based timber harvesting. *Can. J. For. Res.* **2012**, *42*, 821–830. [CrossRef]
47. Affek, A.N.; Zachwatowicz, M.; Sosnowska, A.; Gerlée, A.; Kiszka, K. Impacts of modern mechanised skidding on the natural and cultural heritage of the Polish Carpathian Mountains. *For. Ecol. Manag.* **2017**, *405*, 391–403. [CrossRef]
48. Crawford, L.J. *Soil Disturbance Recovery After Timber Harvests on the Malheur National Forest, Oregon*; University of Idaho: Moscow, ID, USA, 2020.
49. Talbot, B.; Astrup, R. A review of sensors, sensor-platforms and methods used in 3D modelling of soil displacement after timber harvesting. *Croat. J. For. Eng. J. Theory Appl. For. Eng.* **2021**, *42*, 149–164. [CrossRef]
50. Talbot, B.; Rahlf, J.; Astrup, R. An operational UAV-based approach for stand-level assessment of soil disturbance after forest harvesting. *Scand. J. For. Res.* **2018**, *33*, 387–396. [CrossRef]
51. Wang, P.; Hu, Z.; Zhao, Y.; Li, X. Experimental study of soil compaction effects on GPR signals. *J. Appl. Geophys.* **2016**, *126*, 128–137. [CrossRef]
52. Doolittle, J.A.; Brevik, E.C. The use of electromagnetic induction techniques in soils studies. *Geoderma* **2014**, *223*, 33–45. [CrossRef]
53. Kulkarni, S.; Bajwa, S.; Huitink, G. Investigation of the effects of soil compaction in cotton. *Trans. ASABE* **2010**, *53*, 667–674. [CrossRef]
54. Marra, E.; Cambi, M.; Fernandez-Lacruz, R.; Giannetti, F.; Marchi, E.; Nordfjell, T. Photogrammetric estimation of wheel rut dimensions and soil compaction after increasing numbers of forwarder passes. *Scand. J. For. Res.* **2018**, *33*, 613–620. [CrossRef]
55. Kleijnen, J.P. Verification and validation of simulation models. *Eur. J. Oper. Res.* **1995**, *82*, 145–162. [CrossRef]
56. Szabó, B.; Babuška, I. *Finite Element Analysis: Method, Verification and Validation*; John Wiley & Sons Inc.: Hoboken, NJ, USA, 2021.
57. Akay, A.; Sessions, J. Minimizing road construction plus forwarding costs under a constraint of soil disturbance. In Proceedings of the International Mountain Logging and 11th Pacific Northwest Skyline Symposium, Seattle, WA, USA, 10–12 December 2001.

58. Visser, R.; Stampfer, K. Expanding ground-based harvesting onto steep terrain: A review. *Croat. J. For. Eng. J. Theory Appl. For. Eng.* **2015**, *36*, 321–331.
59. Cavalli, R.; Amishev, D. Steep terrain forest operations–challenges, technology development, current implementation, and future opportunities. *Int. J. For. Eng.* **2019**, *30*, 175–181. [CrossRef]
60. Winsen, M.; Hamilton, G. A comparison of UAV-derived dense point clouds using LiDAR and NIR photogrammetry in an Australian eucalypt forest. *Remote Sens.* **2023**, *15*, 1694. [CrossRef]
61. Marra, E.; Laschi, A.; Fabiano, F.; Foderi, C.; Neri, F.; Mastrolonardo, G.; Nordfjell, T.; Marchi, E. Impacts of wood extraction on soil: Assessing rutting and soil compaction caused by skidding and forwarding by means of traditional and innovative methods. *Eur. J. For. Res.* **2022**, *141*, 71–86. [CrossRef]
62. Majnounian, B.; Jourgholami, M. Effects of rubber-tired cable skidder on soil compaction in Hyrcanian Forest. *Croat. J. For. Eng. J. Theory Appl. For. Eng.* **2013**, *34*, 123–135.
63. Naghdi, R.; Solgi, A. Effects of skidder passes and slope on soil disturbance in two soil water contents. *Croat. J. For. Eng. J. Theory Appl. For. Eng.* **2014**, *35*, 73–80.
64. Solgi, A.; Najafi, A.; Sadeghi, S.H. Effects of traffic frequency and skid trail slope on surface runoff and sediment yield. *Int. J. For. Eng.* **2014**, *25*, 171–178. [CrossRef]
65. Picchio, R.; Mederski, P.S.; Tavankar, F. How and how much, do harvesting activities affect forest soil, regeneration and stands? *Curr. For. Rep.* **2020**, *6*, 115–128. [CrossRef]
66. Garten Jr, C.T.; Kang, S.; Brice, D.J.; Schadt, C.W.; Zhou, J. Variability in soil properties at different spatial scales (1 m–1 km) in a deciduous forest ecosystem. *Soil Biol. Biochem.* **2007**, *39*, 2621–2627. [CrossRef]
67. Lin, H.; Wheeler, D.; Bell, J.; Wilding, L. Assessment of soil spatial variability at multiple scales. *Ecol. Model.* **2005**, *182*, 271–290. [CrossRef]
68. Labelle, E.R.; Jaeger, D. Soil compaction caused by cut-to-length forest operations and possible short-term natural rehabilitation of soil density. *Soil Sci. Soc. Am. J.* **2011**, *75*, 2314–2329. [CrossRef]
69. Solgi, A.; Naghdi, R.; Nikooy, M. Effects of skidder on soil compaction, forest floor removal and rut formation. *Madera Y Bosques* **2015**, *21*, 147–155.
70. Kormanek, M.; Banach, J.; Sowa, P. Effect of soil bulk density on forest tree seedlings. *Int. Agrophysics* **2015**, *29*, 67–74. [CrossRef]
71. Ares, A.; Terry, T.A.; Miller, R.E.; Anderson, H.W.; Flaming, B.L. Ground-based forest harvesting effects on soil physical properties and Douglas-Fir growth. *Soil Sci. Soc. Am. J.* **2005**, *69*, 1822–1832. [CrossRef]
72. Kim, H.; Anderson, S.; Motavalli, P.; Gantzer, C. Compaction effects on soil macropore geometry and related parameters for an arable field. *Geoderma* **2010**, *160*, 244–251. [CrossRef]
73. Hatchell, G.; Ralston, C.; Foil, R. Soil disturbances in logging. Effects on soil characteristics and growth of loblolly pine in the Atlantic coastal plain. *J. For.* **1970**, *68*, 772–775.
74. Gomez, A.G.; Powers, R.F.; Singer, M.J.; Horwath, W.R. N uptake and N status in ponderosa pine as affected by soil compaction and forest floor removal. *Plant Soil* **2002**, *242*, 263–275.
75. Solgi, A.; Naghdi, R.; Tsioras, P.A.; Nikooy, M. Soil compaction and porosity changes caused during the operation of Timberjack 450C skidder in northern Iran. *Croat. J. For. Eng. J. Theory Appl. For. Eng.* **2015**, *36*, 217–225.
76. Naghdi, R.; Solgi, A.; Labelle, E.R.; Nikooy, M. Combined effects of soil texture and machine operating trail gradient on changes in forest soil physical properties during ground-based skidding. *Pedosphere* **2020**, *30*, 508–516. [CrossRef]
77. Ferenčík, M.; Dudáková, Z.; Kardoš, M.; Sivák, M.; Merganičová, K.; Merganič, J. Measuring soil surface changes after traffic of various wheeled skidders with close-range photogrammetry. *Forests* **2022**, *13*, 976. [CrossRef]
78. Parajuli, M.; Hiesl, P.; Hagan, D.; Khanal, P. *Logging Operations and Soil Compaction*; Land-Grant Press: Clemson, SC, USA, 2022.
79. Varol, T.; Emir, T.; Akgul, M.; Ozel, H.B.; Acar, H.H.; Cetin, M. Impacts of small-scale mechanized logging equipment on soil compaction in forests. *J. Soil Sci. Plant Nutr.* **2020**, *20*, 953–963. [CrossRef]
80. Groos, A.R.; Aeschbacher, R.; Fischer, M.; Kohler, N.; Mayer, C.; Senn-Rist, A. Accuracy of UAV photogrammetry in glacial and periglacial alpine terrain: A comparison with airborne and terrestrial datasets. *Front. Remote Sens.* **2022**, *3*, 871994. [CrossRef]
81. James, M.R.; Antoniazza, G.; Robson, S.; Lane, S.N. Mitigating systematic error in topographic models for geomorphic change detection: Accuracy, precision and considerations beyond off-nadir imagery. *Earth Surf. Process. Landf.* **2020**, *45*, 2251–2271. [CrossRef]
82. Li, H.; Chen, L.; Wang, Z.; Yu, Z. Mapping of river terraces with low-cost UAS based structure-from-motion photogrammetry in a complex terrain setting. *Remote Sens.* **2019**, *11*, 464. [CrossRef]
83. Liu, X.; Hu, H.; Hu, P. Accuracy assessment of LiDAR-derived digital elevation models based on approximation theory. *Remote Sens.* **2015**, *7*, 7062–7079. [CrossRef]
84. Kameyama, S.; Sugiura, K. Estimating tree height and volume using unmanned aerial vehicle photography and SfM technology, with verification of result accuracy. *Drones* **2020**, *4*, 19. [CrossRef]

85. Foldager, F.F.; Pedersen, J.M.; Haubro Skov, E.; Evgrafova, A.; Green, O. Lidar-based 3d scans of soil surfaces and furrows in two soil types. *Sensors* **2019**, *19*, 661. [CrossRef]
86. Pierzchała, M.; Talbot, B.; Astrup, R. Measuring wheel ruts with close-range photogrammetry. *For. Int. J. For. Res.* **2016**, *89*, 383–391. [CrossRef]
87. Nevalainen, P.; Salmivaara, A.; Ala-Ilomäki, J.; Launiainen, S.; Hiedanpää, J.; Finér, L.; Pahikkala, T.; Heikkonen, J. Estimating the rut depth by UAV photogrammetry. *Remote Sens.* **2017**, *9*, 1279. [CrossRef]
88. Mohieddinne, H.; Brasseur, B.; Gallet-Moron, E.; Lenoir, J.; Spicher, F.; Kobaissi, A.; Horen, H. Assessment of soil compaction and rutting in managed forests through an airborne LiDAR technique. *Land Degrad. Dev.* **2023**, *34*, 1558–1569. [CrossRef]

Disclaimer/Publisher's Note: The statements, opinions and data contained in all publications are solely those of the individual author(s) and contributor(s) and not of MDPI and/or the editor(s). MDPI and/or the editor(s) disclaim responsibility for any injury to people or property resulting from any ideas, methods, instructions or products referred to in the content.